Function and ribosomal localization of aIF6, a translational regulator shared by archaea and eukarya

Dario Benelli[1,2], Stefano Marzi[3], Carmine Mancone[4], Tonino Alonzi[4], Anna la Teana[5] and Paola Londei[1,*]

[1]Dipartimento Biotecnologie Cellulari ed Ematologia, Policlinico Umberto I°, Università di Roma Sapienza, Viale Regina Elena 324, 00161 Roma, [2]DIBIFIM, Università di Bari (Policlinico), Piazza Giulio Cesare, 70127 Bari, Italy, [3]Institut for the Biologie Moleculaire et Cellulare CNRS, 67084 Strasbourg Cedex, France. [4]National Institute for Infectious Diseases 'L. Spallanzani', IRCCS, Via Portuense 292, 00149 Roma and [5]Istituto di Biochimica, Università Politecnica delle Marche, Via Ranieri, 60131 Ancona, Italy

ABSTRACT

The translation factor IF6 is shared by the Archaea and the Eukarya, but is not found in Bacteria. The properties of eukaryal IF6 (eIF6) have been extensively studied, but remain somewhat elusive. eIF6 behaves as a ribosome-anti-association factor and is involved in miRNA-mediated gene silencing; however, it also seems to participate in ribosome synthesis and export. Here we have determined the function and ribosomal localization of the archaeal (*Sulfolobus solfataricus*) IF6 homologue (aIF6). We find that aIF6 binds specifically to the 50S ribosomal subunits, hindering the formation of 70S ribosomes and strongly inhibiting translation. aIF6 is uniformly expressed along the cell cycle, but it is upregulated following both cold- and heat shock. The aIF6 ribosomal binding site lies in the middle of the 30-S interacting surface of the 50S subunit, including a number of critical RNA and protein determinants involved in subunit association. The data suggest that the IF6 protein evolved in the archaeal–eukaryal lineage to modulate translational efficiency under unfavourable environmental conditions, perhaps acquiring additional functions during eukaryotic evolution.

INTRODUCTION

Several translation factors are shared selectively by the Archaea and the Eukarya. One of these is the small monomeric protein (about 25 kDa) called eIF6 in eukarya and aIF6 in archaea. In eukaryotes, eIF6 was identified originally as a ribosome anti-association factor, capable of binding specifically to the 60S subunits inhibiting their association with the 40S particles; it was therefore classified as a translation initiation factor (1,2). Subsequent studies have, however, cast doubts on the real function of the protein. Genetic analyses performed on yeast strains defective in eIF6 showed that the factor is essential for cell growth and viability. However, lack of eIF6 did not impair translational initiation, but lowered the amount of 60S ribosomal subunits because of impaired processing of 35S and 27S pre-rRNA precursors (3,4). Therefore, yeast eIF6 seemed to be a factor for ribosome biogenesis, involved in some late step of 60S subunit maturation (5). The release of yeast eIF6 from cytoplasmic pre-60S subunits required the combined action of two factors, the GTPase Efl1 and Sdo1(6–9).

However, recent studies in mammalian cells have revived the idea that eIF6 may play an important role in the regulation of protein synthesis initiation. In human cells, at least 50% of eIF6 is localized in the cytoplasm, both in free form and associated with the 60S ribosomal subunits; 60S ribosomes carrying eIF6 are translationally inactive (10). The release of human eIF6 from the 60S particles requires the phosphorylation of the factor, which is in turn controlled by kinases activated by mitogenic signals (10). In this view, eIF6 would be a factor capable of modulating the efficiency of translational initiation (and hence general translation) by regulating ribosome availability. The idea that the factor may have an important role in translational control is also strongly supported by the recent findings that in both cultured mammalian cells and in *Caenorhabditis elegans* eIF6 is essential for miRNA-induced genetic silencing (11) and that heterozygous knockout mice for the eIF6 gene have a defect in translational initiation (12).

*To whom correspondence should be addressed. Tel: +39 06 4940463; Fax: +39 06 4462891; Email: londei@bce.uniroma1.it

The presence in Archaea of an orthologue of eIF6 (aIF6) offers a precious opportunity to elucidate the function of this interesting protein by placing it in a wider biological context. Archaeal and eukaryal IF6 proteins share a considerable degree of homology in their primary sequence and have essentially the same tertiary folding (13), suggesting that they share a core function conserved in the eukaryal/archaeal line.

In this work, we have studied experimentally for the first time the functional properties of archaeal (*Sulfolobus solfataricus*) IF6. We show that aIF6 acts as a translational inhibitor by binding specifically to the large ribosomal subunit and impairing the formation of 70S particles. We have mapped the ribosomal binding site of aIF6 and present a structural model of the aIF6/50S subunit complex showing how it accounts for the ribosome anti-association activity of the protein. As aIF6 is over-expressed under stress conditions, its probable biological role is that of negatively regulating protein synthesis under unfavourable circumstances.

MATERIALS AND METHODS

Cloning of the *S. solfataricus* aIF6 and L14 genes and isolation of the recombinant proteins

The aIF6 gene was PCR-amplified from *S. solfataricus* genomic DNA using a forward primer containing an NdeI site (5′-TTTTTTCATATGAATCTGCAAAGGTT ATC-3′) and a reverse primer containing a XhoI site (5′-TTTTTCTCGAGTTCACCTAATGCTTTTTGAA-3′). The amplification product was inserted into the pET-22b(+) plasmid (Novagen) to yield the recombinant pET-aIF6 (6His) expression plasmid, which was sequenced and inserted into *Escherichia coli* BL21 (DE3) cells. aIF6 expression was induced for 4 h with 1 mM IPTG at an OD_{600} of 0.6. After cell lysis, the supernatant was heated for 10 min at 70°C and centrifuged to precipitate mesophilic *E. coli* proteins. Recombinant aIF6 was purified to homogeneity by affinity chromatography on Ni–NTA agarose followed by ionic-exchange chromatography on DEAE column (HiTrap DEAE FF, Amersham Biosciences). aIF6 was eluted in 20 mM Tris/HCl pH 8.0, 100 mM NH_4Cl, dialysed against storage buffer, (20 mM Tris/HCl pH 7.4, 20 mM NH_4Cl, glycerol 10%), and stored at –80°C in aliquots. Antibodies against aIF6 were raised in rabbit by Eurogentec, Belgium.

The *S.solfataricus rpl14AB* gene was amplified using a forward primer containing an NdeI site (5′-TTTTTTCA TATGTCAGAAAAGATTCAAGTTTTAGG-3′) and a reverse primer containing a XhoI site (5′-TTTTTCTC GAGCACCACCAATGTAGCGAGACTAGA-3′). The amplification product was cloned and the protein expressed as described above for aIF6. To recover recombinant L14, the cell pellet was re-suspended in denaturing lysis buffer (100 mM NaH_2PO_4, 10 mM Tris–HCl, 8 M Urea, pH 8) at 5 ml per gram wet weight and stirred for 60 min at room temperature. The lysate was clarified by centrifugation at 10 000 *g* for 30 min. His_6-aL14 was purified from the lysate incubating over-night on Ni-NTA agarose resin (Qiagen) at room temperature, washing the resin three times with wash buffer (100 mM NaH_2PO_4, 10 mM Tris–HCl, 8 M Urea, pH 6.3) and eluting the recombinant protein four times with 0.5 ml elution buffer pH 5.9 (100 mM NaH_2PO_4, 10 mM Tris–HCl, 8 M Urea, pH 5.9) followed by four times with 0.5 ml elution buffer pH 4.5 (100 mM NaH_2PO_4, 10 mM Tris–HCl, 8 M Urea, pH 4.5). Small aliquots of the elution fractions were analysed by SDS–PAGE followed by the Coomassie staining of the gel. The fractions containing His_6-aL14 were collected and dialysed against storage buffer (100 mM KCl, 20 mM HEPES-OH, pH 6.8, 4 mM $MgCl_2$, 5% glycerol). The concentration of the samples was determined by the Bradford assay and aliquots of the protein were stored at –80°.

Preparation of cell extracts and ribosomes

Cell lysates, 70S ribosomes and 30S and 50S ribosomal subunits were obtained from frozen *S. solfataricus* cells as described previously (14).

In vitro translation

Cell-free systems programmed for *in vitro* translation were prepared as described by Condò *et al.* (1999). The effect of aIF6 on *in vitro* translation was assayed by adding 5, 10 or 20 pmol of the factor, or of the control unrelated protein SUI1, to the reaction mixture, in a final volume of 25 μl and incubating the samples for 30 min at 70°C. At the end of the incubation 10 μl of the mixtures were withdrawn and electrophoresed on 15% acrylamide-SDS minigels. The radioactive bands were detected and quantified using either an Instant Imager apparatus (Packard) or an X-ray film.

To check the effect of aIF6 on the formation of 70S subunits, translational mixtures containing 5, 10 and 20 pmol of aIF6 were incubated as above, except that the samples contained 20 mM triethanolamine (TEA)/HCl pH 7.4 instead of 20 mM Tris/HCl pH 7.4. At the end of the reaction fixation on ice with 0.5% formaldehyde for 30 min was performed and the samples were layered on linear, 10 to 30% sucrose gradients containing 10 mM KCl, 20 mM, 20 mM TEA/HCl pH 7.4 and 10 mM $MgCl_2$. The gradients were centrifuged at 36 000 r.p.m. for 4 h in a Beckman SW41 rotor and unloaded while monitoring absorbance at 260 nm.

Analysis of aIF6 levels under different growth conditions

The *S. solfataricus* cells were aerobically cultivated at 80°C in DSM 182 medium at pH 3.0. Cells harvested at different densities were re-suspended with extraction buffer (20 mM Tris/HCl pH 7.4, 10 mM $MgCl_2$, 40 mM NH_4Cl and 1 mM DTT) and disrupted by three cycles of incubation at 37°C/liquid nitrogen for 5 min. The total protein concentration in the cell extract was measured by the Bradford assay.

Cold and heat-shock treatments were performed as follows. Cells grown at 80°C to the late exponential phase were transferred to either 65°C or 90°C. After 30 min, the cells were harvested and the lysates prepared as described above.

In all cases, the lysates were fractionated by SDS–PAGE; the presence of aIF6 was revealed by western blotting and quantified with the Image J software; the data were normalized using the reference protein L7ae, revealed with the specific antibodies.

Interaction of aIF6 with ribosomes

The binding of aIF6 to ribosomal subunits was investigated by incubating purified *S. solfataricus* ribosomes (100 pmol) with 200 pmol of His-tagged aIF6 in 50 μl (final volume) of 50 mM NH_4Cl, 10 mM $MgCl_2$, 20 mM Tris/HCl pH 7.4 for 10 min at 65°C. The samples were fractionated on linear, 10–30% sucrose gradients which were run and unloaded as described above, collecting 0.5-ml fractions. These were supplemented with 5 vol of acetone, and the precipitated proteins were re-suspended in 20 μl of SDS-sample buffer, separated by SDS–PAGE and electroblotted to nitrocellulose membrane. The presence of aIF6 was probed with either anti-aIF6 polyclonal rabbit antibodies or anti-His monoclonal mouse antibodies (Qiagen) and detected by ECL.

To measure the affinity of aIF6 for the 50S ribosomes, binding experiments were performed essentially as described in (15) in a reaction volume of 60 μl which contained 20 mM Tris–HCl (pH 7.4), 50 mM NH_4Cl, 10 mM $MgCl_2$, 28 pmol of recombinant aIF6 and increasing amounts of 50S ribosomal subunits to achieve the aIF6/50S ratios indicated in Figure 2. After incubation at 65°C for 10 min the reaction volume was increased by addition of 30 μl of the same buffer containing 30% sucrose. Samples were then centrifuged for 45 min at 100 000 r.p.m. in a Sorvall ultracentrifuge (RC M120 GX, rotor S100AT3-205) and 20 μl aliquots from the supernatants were subjected to SDS–PAGE followed by western blot analysis to determine the amount of unbound protein.

Chemical probing

Fifty picomoles of purified *S. solfataricus* 50S ribosomal subunits were incubated, either alone or in the presence of 200 pmol of recombinant aIF6, in 100 μl of 50 mM NH_4Cl, 10 mM $MgCl_2$, 80 mM K-HEPES pH 7.8 for 10 min at 65°C. Modification was carried out for 5 min at 65°C, by addition of the following reagents: dimethylsulphate (DMS, Kodak) to probe A at N1, C at N3, kethoxal (ICN) to probe G at N1 and N2, and 1-cyclohexyl-3-(2-morpholinoethyl) carbodiimide methoptoluene sulphonate (CMCT, Sigma) to probe U at N3 and G at N1 (16). After modification, ribosomal RNA was extracted and the modified residues identified by primer extension analysis as described (16,17), using a set of 20–21-mer oligonucleotides complementary to 23S regions spaced about 200 nt apart. The radioactive bands in the gels were quantified using the Image J software, on four independent replicate experiments.

Immunoprecipitation procedures

Immunoprecipitation of aIF6 from crude lysates (5 mg) or purified 50S ribosomal subunits was preceded by a pre-clearing step during which 30 μl of 50% protein A-Sepharose CL-4B (Amersham Biosciences) were

incubated for 1 h at 4°C in 500 μl of cell lysate in 20 mM Tris/HCl pH 7.4, 40 mM NH_4Cl, 10 mM $MgCl_2$. At the same time, another 30 μl of 50% protein A-Sepharose was combined with either 2 μl of anti-aIF6 polyclonal rabbit serum or 4 μl of pre-immune serum in 500 μl of PBS 1 × for 1 h at 4°C. At the end of incubation, the antibody-conjugated resin was washed two times with cold extraction buffer (20 mM Tris/HCl pH 7.4, 40 mM NH_4Cl, 10 mM $MgCl_2$) and mixed with the pre-cleared samples for 3 h at 4°C. Immunocomplexes were washed thrice with cold wash buffer (0.1% Triton X-100, 50 mM Tris/HCl pH 7.4, 300 mM NaCl, 5 mM EDTA), once with cold 1 × PBS, eluted and denatured by heating for 4 min at 95°C in non-reducing Laemmli buffer. Samples were then resolved by SDS–PAGE.

To analyse the direct interaction of aIF6 and aL14, 40 pmol of aIF6 His-tagged and 40 pmol of either aL14 or aL7A His-tagged, were incubated at 65°C for 5 min in binding buffer (20 mM NH_4Cl, 12 mM HEPES-OH pH 7, 40 mM KCl, 8 mM $MgCl_2$, 2% glycerol) to a final volume of 50 μl. Complexes were immunoprecipitated overnight at 4°C with either 2 μl of anti-aIF6 antibodies or 4 μl of pre-immunized rabbit serum bound to 30 μl of 50% protein A-Sepharose CL-4B (GE Healthcare) resin. Immunocomplexes were washed thrice with cold wash buffer (0.1% Triton X-100, 50 mM Tris/HCl pH 7.4, 300 mM NaCl, 5 mM EDTA), once with cold 1 × PBS, eluted and denatured by heating for 5 min at 95°C in reducing Laemmli buffer. Proteins were separated by SDS–PAGE and then electroblotted to nitrocellulose membrane. The His-tagged proteins were visualized by probing the membrane with antibodies anti-His (Qiagen) and detected by ECL.

Mass spectrometry (MS)

Immunoprecipitated proteins were resolved on a 12%T-3.3%C SDS–PAGE separating gel (1 + 18 + 18 mm), revealed by Sypro Ruby staining and visualized using a Typhoon 9200 laser scanner (GE Healthcare). Proteins were excised from the gel using Investigator ProPic spot picker (Genomic Solutions) and transferred to small tubes (0.2 ml). Protein-containing gel pieces were destained with 50 μl of 0.1 M ammonium bicarbonate (5 min at RT). After two washes with 50% acetonitrile/0.05 M ammonium bicarbonate, gel plugs were shrunk by addition of 100% acetonitrile. The dried gel pieces were re-swollen with 4.5 ng/μl trypsin in 50 mM ammonium bicarbonate and digested overnight at 37°C. Peptides were concentrated with ZipTipμC18 pipette tips (Millipore). Co-elution was performed directly onto a MALDI target with 1 μl of α-cyano-4-hydroxycinnamic acid matrix (5 mg/ml in 50% acetonitrile, 0.1% TFA).

Proteins were identified by Matrix Assisted Laser-Desorption Ionization (MALDI)-MS and MALDI-MS/MS (4700 Proteomics Analyzer; Applied Biosystems). Data were acquired in positive MS reflector mode. Five peptides (ABI4700 Calibration Mixture; Applied Biosystems) were used as calibration standards. Mass spectra were obtained from each sample by 30 sub-spectra accumulation (50 laser shots each) in a 750 to 4000

mass range. Five signal-to-noise best peaks of each spectrum were selected for MS/MS analysis. For MS/MS spectra, the collision energy was 1 keV and the collision gas was air. The interpretation of both the MS and MS/MS data was carried out by using the GPS Explorer software (Version 1.1, Applied Biosystems), which acts as an interface between the Oracle database containing raw spectra and a local copy of the MASCOT search engine (Version 1.8). Peptide mass fingerprints obtained from MS analysis were used for protein identification in the NCBI non-redundant database. All peptides mass values were considered monoisotopic and mass tolerance was set at 50 p.p.m. One missed cleavage site was allowed, cysteines were considered carboamidomethylated, methionine was assumed to be partially oxidized and serine, threonine and tyrosine partially phosphorylated. Mascot (Matrix Science) scores >61 were considered significant ($P < 0.005$). For MS/MS analysis, all peaks with a signal-to-noise ratio >5 were searched against the NCBI database using the same modifications as the MS database, with a fragment tolerance <0.3 Da.

Modelling of 50S subunits and aIF6

A model of *Haloarcula marismortui* 50S has been build with the implementation of H69. The atomic coordinates of the *H. marismortui* 50S have been taken from the 1JJ2.pdb file (18). The model of H69 has been produced using the programs Assemble (http://www.bioinformatics. org/assemble/wiki/index.php/Main_Page) and Pymol (http://www.pymol.org), where prokaryotic H69 from *E. coli* 70S structure (file 2I2V.pdb) (19) has been used as a template. The homology model of *S. solfataricus* aIF6 has been realized using the structure of the homologous *Methanococcus jannaschii* aIF6 (13). Pair-wise sequence alignment between *M. jannaschii* aIF6 (pdb **1g61A;** 13) and *S. solfataricus* aIF6 has been improved by multiple sequence alignment (PipeAlign at http:// igbmc.u-strasbg.fr/PipeAlign/) (20) and further manually adjusted before generating the homology model. Both the SwissProt server (21) and the program MODELLER (22) have been used producing substantially equivalent results with a structure-based superposition giving a root mean square deviation of only 0.816 Å.

RESULTS

Molecular cloning and expression of the *S. solfataricus* aIF6 gene

The *S. solfataricus* aIF6 was cloned by PCR amplification on genomic DNA, inserted in the expression plasmid pET/22b(+), produced in *E. coli* BL21(DE3) and purified from cell extracts by a three-step method, involving differential thermal denaturation, affinity chromatography and ion-exchange chromatography. This procedure yielded a recombinant aIF6 that migrated as a single sharp band free of detectable contaminants even after silver staining (Figure S1). The cloned aIF6 gene encodes a protein of 231 amino acids with a predicted molecular mass of 25 kDa. This value is in a close agreement with the experimentally observed size of our purified archaeal aIF6.

Endogenous aIF6 is specifically bound to 50S ribosomal subunits

To determine the cellular localization of aIF6, *S. solfataricus* whole-cell extracts were fractionated on density gradients. The gradient fractions were monitored for their absorbance at A_{260} and probed by western blotting with polyclonal antibodies raised against the recombinant aIF6. As illustrated in Figure 1a, the aIF6 antiserum recognized a single polypeptide of the expected size, the majority of which was localized in the fractions containing the 50S ribosomal subunits. The aIF6/50S ratio was estimated by performing densitometric measurements on western blots made on known increasing amounts of purified 50S subunits; it turned out to be about 1:10 (data not shown). Thus, in *S. solfataricus* cells aIF6 is specifically associated with 50S ribosomes in sub-stoichiometric amounts.

To determine the behaviour and localization of aIF6 during translation, density gradient fractionations were next performed on lysates programmed for protein synthesis as described by (23). The programmed lysates were incubated at 70°C for 30 min to activate translation, and were then fixed with formaldehyde to stabilize 70S ribosomes which are easily dissociated in *S. solfataricus* (14). As shown in Figure 1b, ribosome-bound aIF6 was again exclusively localized on the 50S subunits; however, the amount of free factor increased substantially, suggesting that activation of translation triggered the dissociation of aIF6 from the 50S subunits. Interestingly, the release of aIF6 was accompanied by the evident appearance of a slower-migrating form of the protein, barely appreciable in 'resting' lysates. We investigated whether the latter derived from site-specific phosphorylation as described for the eukaryotic factor. This seemed not to be the case, as treatment with phosphatases, though effective in dephosphorylating other *S. solfataricus* proteins, did not affect either the mobility or the appearance of the slower aIF6 band (Figure S2). We concluded therefore that aIF6 release from the 50S subunit is accompanied by an as yet uncharacterized chemical modification of the factor.

aIF6 inhibits *in vitro* translation impairing 70S particles formation

The specific binding of aIF6 to the 50S ribosomal subunits, and its absence from 70S particles, suggested that the archaeal protein, as its eukaryal counterpart, behaved as a ribosome anti-association factor (1,10). To verify this surmise, we asked whether the addition of recombinant aIF6 to an *in vitro* translation system affected the synthesis of a reporter protein. Preliminarily, we checked the ribosome binding pattern of the recombinant factor, by adding an aliquot of the purified protein to the cell lysates and fractionating the samples through density gradients. The results (Figure 2a) revealed that recombinant aIF6 behaved as its native counterpart in interacting specifically with the 50S ribosomal subunits. To assess the stoichiometry of binding, increasing amounts of purified 50S subunits, free of detectable endogenous aIF6, were incubated with a fixed amount of aIF6 and the resulting 50S/IF6 complexes were separated from the unbound protein
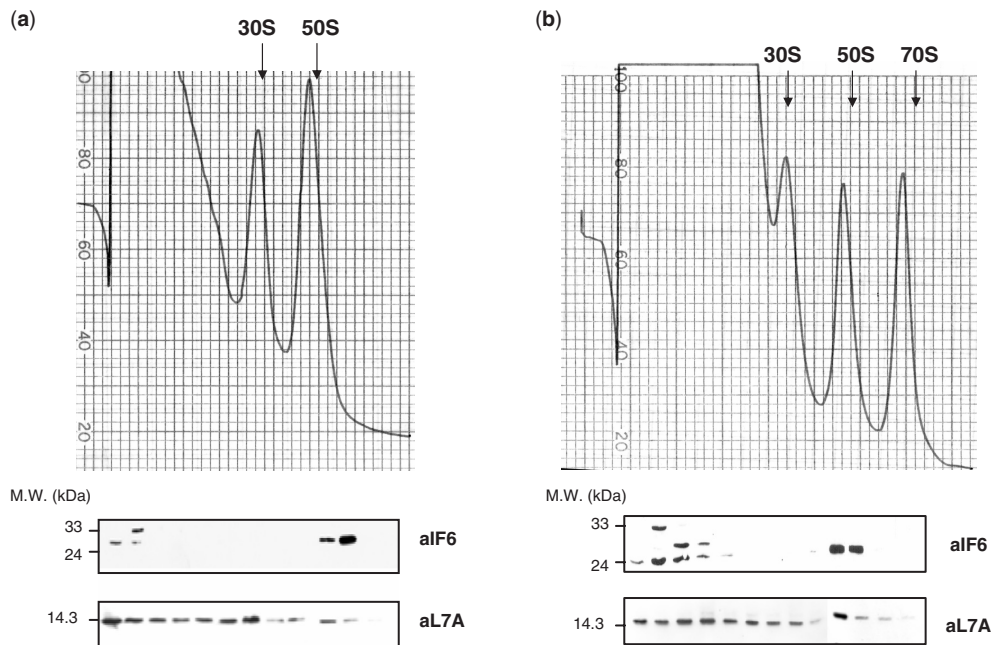
Figure 1. *Sulfolobus solfataricus* aIF6 interacts specifically with the 50S subunits. (**a**) Density gradient fractionation of crude, non-incubated, cell lysates. (**b**) Density gradient fractionation, after fixation with HCHO, of cell lysates programmed for translation and incubated at 70°C for 30 min. The distribution of aIF6, shown at the bottom of each gradient profile, was revealed by western blotting of the individual fractions with the anti-aIF6 antibodies. The distribution of the control protein L7ae, which is localized both in the cytoplasm and on the 50S ribosomal subunit, is also shown.

by ultracentrifugation. The amount of unbound aIF6 in each sample was estimated and quantified by western blotting and densitometry. The final aIF6/50S ratio was 1:1, thus revealing that aIF6 has a single ribosomal binding site which remains fully accessible on the entire cellular pool of 50S ribosomes (Figure 2b). The affinity constant of aIF6 for the 50S subunits calculated from the binding curves was approx. $1 \times 10^7\,M^{-1}$; this value is in the same order of magnitude as that calculated for IF3, the bacterial initiation factor with ribosome anti-associating properties (24).

The effect of aIF6 on translation was assayed next. *S. solfataricus* lysates programmed for translation with a reporter mRNA (23) were supplemented with increasing amounts of recombinant aIF6. Two reporter mRNAs were used in this experiment: one had a 5′UTR including a Shine-Dalgarno motif, while another was leaderless. As translation of leadered and leaderless mRNAs is initiated with different mechanisms in archaea (25), it was important to assess whether only one, or both, were affected by aIF6. As shown in Figure 3a, the translation of both mRNAs was inhibited proportionally to the amount of aIF6 added to the system, while being unaffected by the addition of another putative translation factor, the protein termed aSUI1 (or aIF1). Fractionation of the translational mixtures on density gradients showed that the amount of 70S monomers decreased with increasing aIF6 (Figure 3b), thus suggesting that translational inhibition was due to impaired subunit association.

aIF6 is uniformly expressed in the cell cycle but is over-expressed under stress conditions

To get some insight into the cellular function of aIF6, we asked whether the protein was differentially expressed
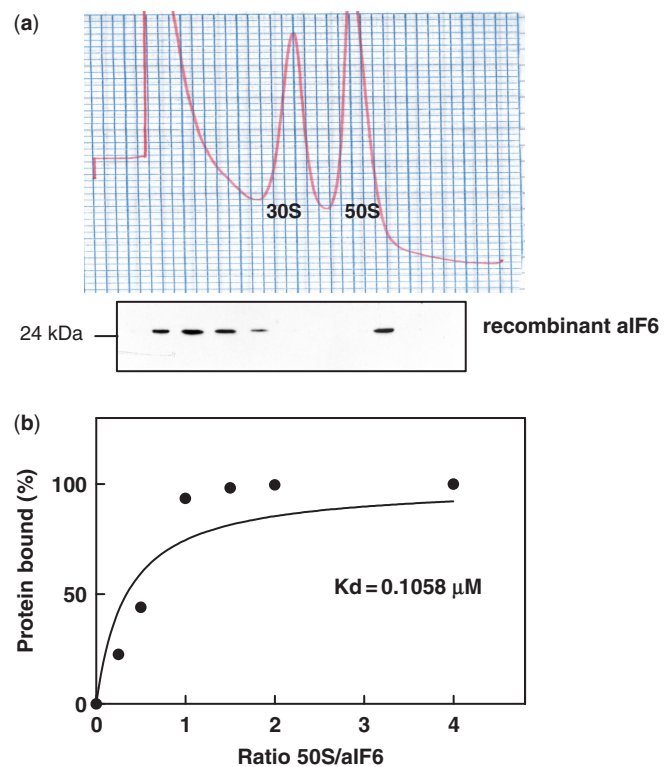

Figure 2. aIF6 has a single binding site on the 50S subunits. (**a**) Sucrose gradient fractionation of a preparation of *S. solfataricus* ribosomes incubated for 10 min at 65°C with an excess of recombinant aIF6. The presence of a IF6 in the gradient fractions was revealed by western blotting with the specific antibodies. (**b**) Binding curve of aIF6 to 50S ribosomes, showing saturation at a 1:1 protein/50S ratio. The amount of ribosome-bound aIF6 was evaluated as described in 'Materials and methods' section.
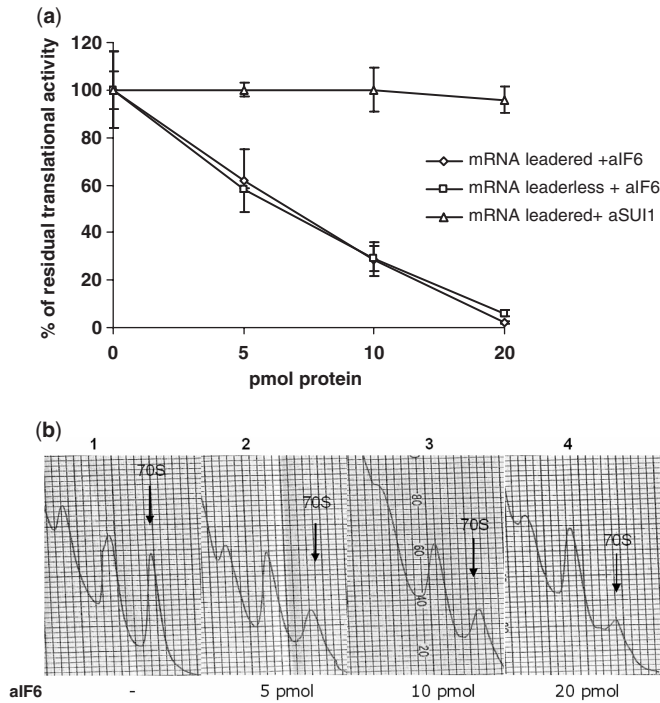
(a)

(b)

Figure 3. aIF6 blocks translation by inhibiting ribosomal subunit association. (**a**) Progressive inhibition of the translation of two reporter mRNAs, one leadered and one leaderless, upon addition of increasing amounts of recombinant aIF6 to a protein-synthesizing cell-free system. Lack of inhibition by the control protein aSUI1 is also shown. Each experimental point represents the average of three replicate experiments. (**b**) Density gradient fractionation of translation mixtures containing increasing amounts of recombinant aIF6 as indicated.

during the cell-cycle or in response to environmental changes. First, we evaluated the amount of aIF6 produced in different phases of cell growth, namely early exponential (0.2 OD_{660}), mid exponential (0.4 OD_{660}) and late exponential (0.8 OD_{660}). No substantial differences in aIF6 abundance were detected, suggesting that the expression of the factor is not cell-cycle regulated (Figure 4). Next, *S. solfataricus* cells grown to late exponential phase at the normal temperature of 80°C were subjected to both cold-shock and heat-shock, by transferring the cultures for 30 min at 60°C and 90°C, respectively. Both treatments stimulated aIF6 expression about 3-fold (Figure 4). A similar result was reported following microarray studies on the whole genome of *S. solfataricus*, where aIF6 was found to be over-expressed about 3-fold following 1 h heat-shock at 90°C (26).

aIF6 interacts with ribosomal protein L14

To identify proteins interacting with aIF6, immunoprecipitation experiments were performed on both whole-cell lysates and isolated ribosomes. As shown in Figure 5, several specific bands appeared in both samples. The best resolved bands were identified by MALDI-TOF/TOF analysis. Most of them turned out to be large ribosomal subunit proteins, some of which were clearly identifiable only in the ribosomal immunoprecipitates (Figure 5, lane 5). These proteins were mostly present in tiny amounts and probably derived from whole 50S particles precipitating along with bound aIF6.

One protein, however, was specially abundant in the immunoprecipitates from both lysates and ribosomes,
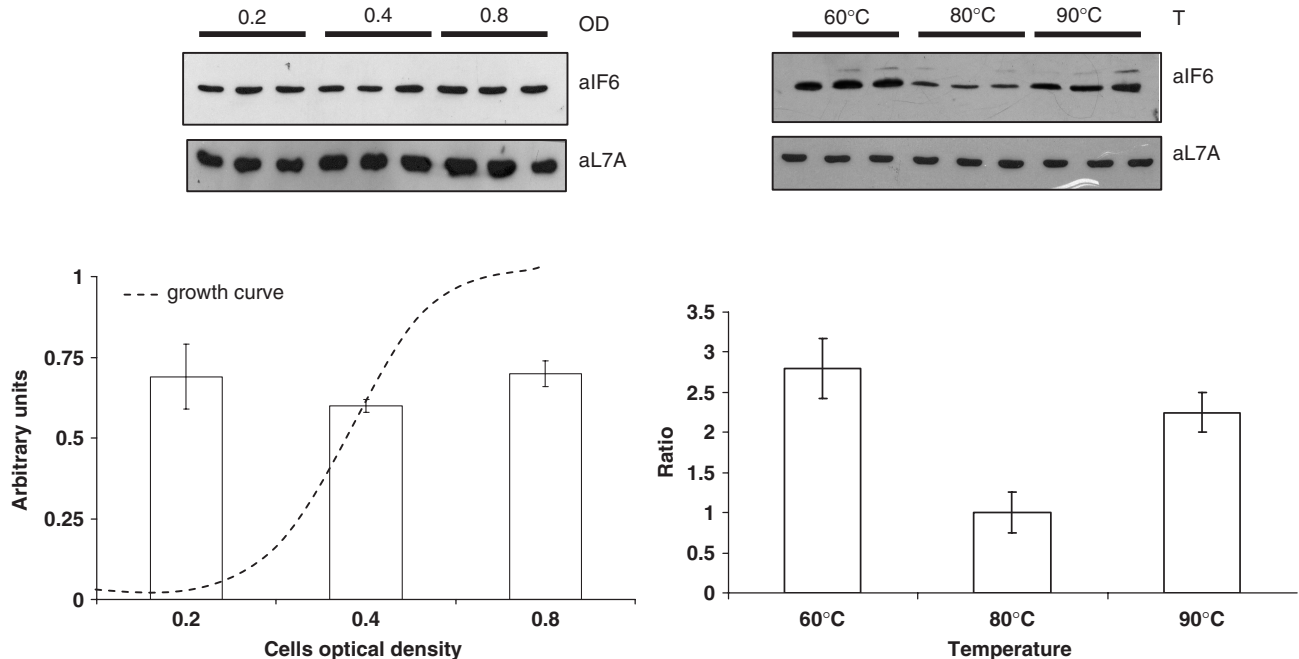

Figure 4. Expression of aIF6 in the cell cycle and upon thermal stress. Left: *S. solfataricus* cell cultures were grown to the indicated OD_{660}; the cell lysates were electrophoresed and probed with the anti-aIF6 antibodies. Three replicate experiments were averaged, and the data were normalized using protein L7ae as the reference. Right: cells grown to the late exponential phase at 80°C were transferred for 30 min at 65°C for cold-shock and at 90°C for heat-shock; a control aliquot was left untreated. The amount of aIF6 in the cell lysates was evaluated by western blotting with the anti-aIF6 antibody and normalized using L7ae as the reference. The numbers on the vertical axis represent the fold increase in aIF6 amount relative to the 80°C value; each value represents the average of three replicate experiments.
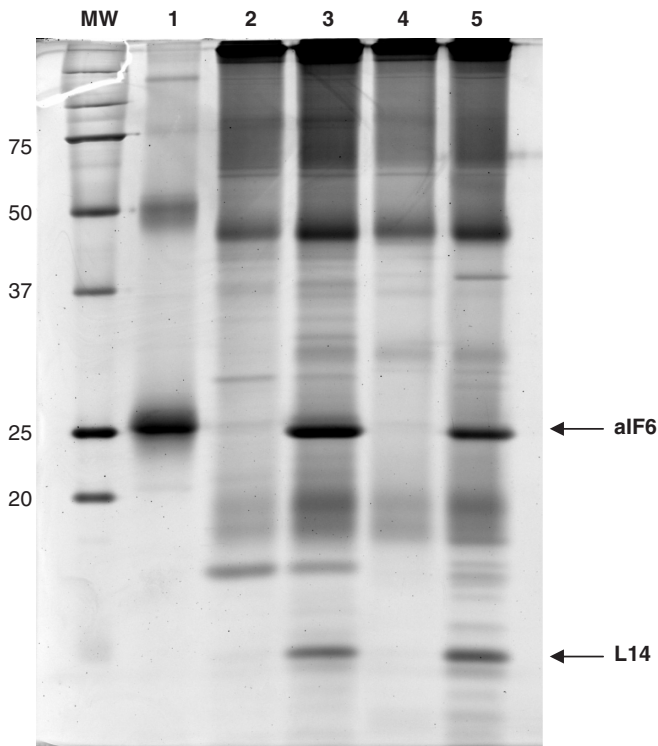
Figure 5. aIF6 interacts with ribosomal protein L14. Sypro-ruby-stained SDS–PAGE showing the protein bands recovered after immunoprecipitation of whole cell lysates or purified 50S subunits with the anti-aIF6 antibodies. Lane 1, control with recombinant aIF6; lanes 2 and 3, whole-cell lysates treated, respectively, with pre-immune serum or anti-aIF6 antibodies; lanes 4 and 5, 50S subunits treated, respectively, with pre-immune serum or anti-aIF6 antibodies. The bands containing aIF6 and L14 (indicated by the arrows) were unambiguously identified by MALDI-TOF/TOF.

and was the only one present in roughly equimolar amounts with IF6 (Figure 5, lanes 3 and 5). It had a molecular weight of about 10 kDa and was unambiguously identified by MALDI-TOF/TOF as ribosomal protein L14p. On the whole, the data suggested that L14 interacts directly with aIF6 forming a complex that is partly detached from the ribosome following treatment with the anti-aIF6 antibodies.

That aIF6 does interact with rpL14 even off the ribosome was established by co-immunoprecipitation experiments. Purified recombinant aIF6 and aL14 were incubated for 5 min at 65°C; the incubation mixtures were treated with the anti-aIF6 antibodies and the proteins in the immunoprecipitate were separated by SDS–PAGE and revealed by western blotting with antibodies directed against the His-tag possessed by both recombinant proteins. The results (Figure 6a) showed that L14 co-immunoprecipitated with aIF6. The specificity of this *in vitro* interaction was assessed with control experiments showing that another *S.solfataricus* large subunit protein, L7ae, similar in size to L14, failed to co-immunoprecipitate with aIF6 (Figure 6b).

aIF6 binds to the domain IV of *S. solfataricus* 23S ribosomal RNA

To determine the topographical localization of aIF6 on the 50S ribosomal subunits the region of 23S RNA involved in aIF6 binding was mapped by means of chemical modification/primer extension experiments. Purified, high-salt washed 50S subunits were incubated at 65°C with an excess of recombinant aIF6 to fully occupy the factor's binding site. Void 50S subunits and aIF6/50S complexes were then treated with base-modifying
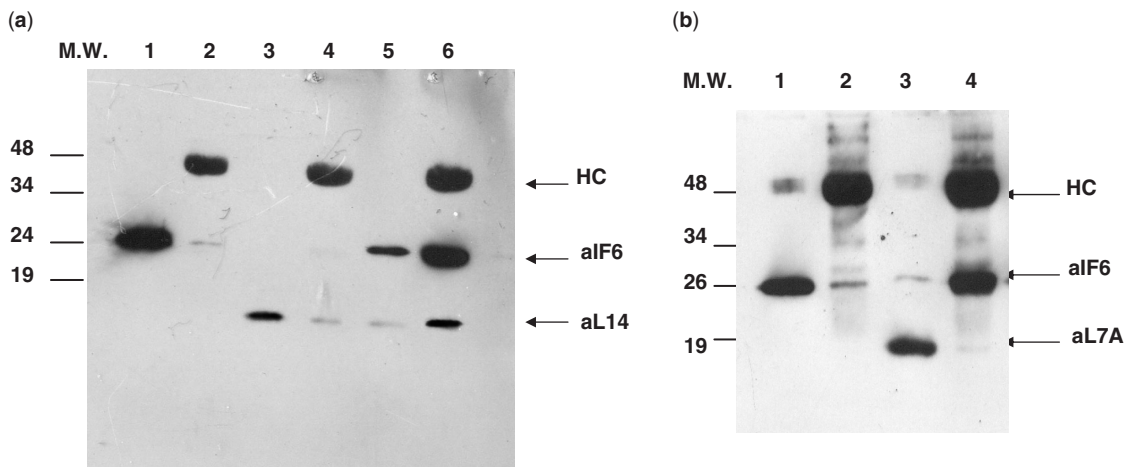

Figure 6. Recombinant aIF6 and aL14 interact specifically *in vitro*. (**a**) Recombinant aIF6 and aL14 were incubated, separately and together, as described in the methods; the samples were treated with the anti-aIF6 antibodies or the correspondent pre-immune serum, electrophoresed and immunostained with the anti-His antibodies. Lanes 1 and 2, supernatant and precipitate, respectively, of a sample containing aIF6 treated with pre-immune serum; lanes 3 and 4, supernatant and precipitate, respectively, of samples containing aL14 treated with anti-aIF6 antibodies; lanes 5 and 6, supernatant and precipitate, respectively, of samples containing both aL14 and aIF6 treated with the anti-aIF6 antibodies. (**b**) Immunoprecipitation with the anti-aIF6 antibodies of samples containing aIF6 and the control ribosomal protein L7ae. Lanes 1 and 2, supernatant and precipitate, respectively, of samples containing aIF6 treated with the pre-immune serum; lanes 3 and 4, supernatant and precipitate, respectively, of samples containing aIF6 and L7ae treated with the anti-aIF6 antibodies. Staining was with the anti-His antibodies. HC: antibody heavy chain.
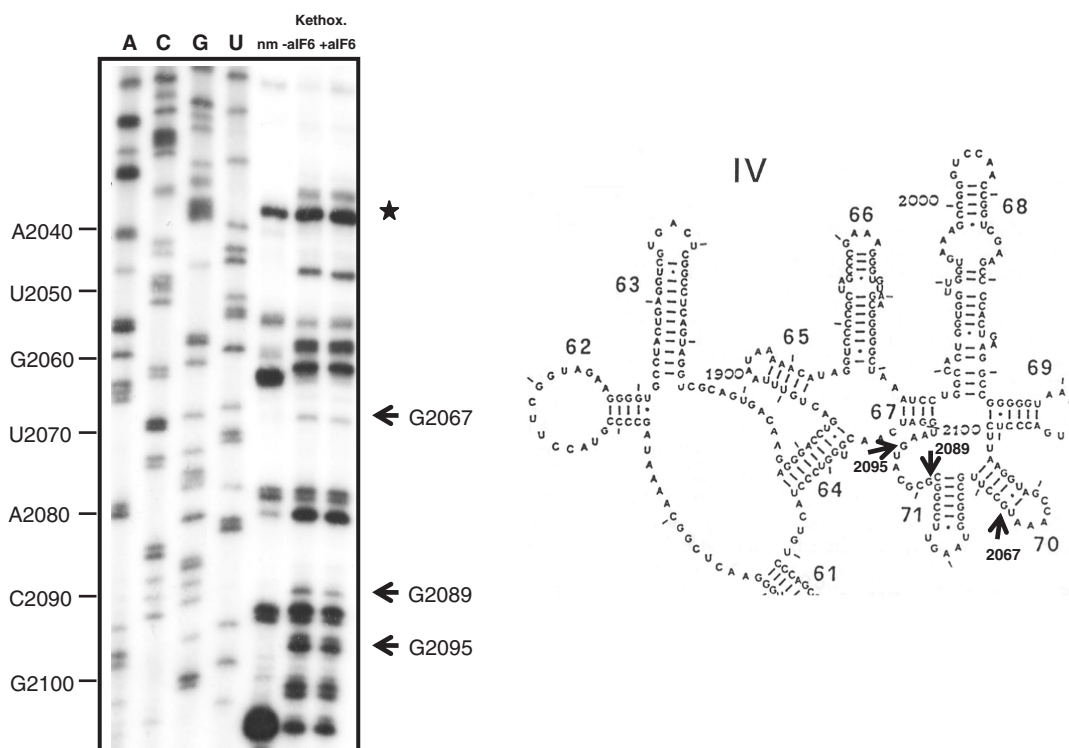
Figure 7. Identification of the 23S rRNA bases protected by bound aIF6. The left panel displays the autoradiography of a sequencing gel including samples of untreated 50S subunits (nm) and kethoxal-modified 50S subunit in the absence (-aIF6) or in the presence (+aIF6) of the recombinant aIF6 protein. A,C,G,U lanes show the sequence of the relevant rRNA region. The nucleotides significantly protected against modification by bound aIF6 are indicated by arrows; the reference band used for normalization is indicated by an asterisk. The primer used was complementary to region 2178–2198 of *S. solfataricus* 23S rRNA. The right panel shows a diagram of the secondary structure of *S.solfataricus* 23S rRNA domain IV (28), where the modified guanines are indicated by arrows.

reagents: DMS to probe As, kethoxal to probe Gs, and CMCT to probe Us (27). These reagents modify exposed, single-stranded bases in the rRNA; bound aIF6 will protect from modification the bases located in, or near, its binding site. The comparison between the modification pattern of void 50S subunits and that of aIF6/50S complexes allows to locate the ribosomal binding site of the factor.

As shown in Figure 7, the presence of aIF6 protected from chemical modification several nucleotides all located within domain IV of 23S RNA and clustered in the region including helices 69, 70 and 71 according to the *S. solfataricus* 23S structural model (28). The most reproducible protections regarded nucleotides G2067 in the distal tract of helix 70 and nucleotides G2089 and G2095 in the loop preceding helix 71 (Figure 7 and Supplementary Table 1). No bases significantly protected by aIF6 against modification by either DMS, kethoxal or CMCT were identified in any other region of *S. solfataricus* 23S rRNA.

It should be noted that the region spanning nucleotides 2058–2071, although depicted as a helix (helix 70) in *S. solfataricus* 23S structure, is more likely to be organized as an extended loop, similar to what happens in other organisms such as *H. marismortui* or *E. coli*. In any event, the distal tract of *S. solfataricus* helix 70, comprising one AU and one GU base pair, is certainly weak enough to be accessible to the base-modifying reagents.

Modelling of the aIF6 binding site on 50S ribosomal subunits

To structurally interpret our data and to dock *S. solfataricus* aIF6 on the archaeal 50S subunit we produced models for both the protein and the ribosome. The only available structure for archaeal 50S subunit has been solved by X-ray analysis of *H marismortui* 50S crystals (29). In this structure several regions have been found to be disordered; these comprise all of helix H1, the distal end of helix H38, helix H43/H44 to which ribosomal protein L11 binds, the loop end of stem–loop H69, and helix H76/H77/H78, which constitute the L1-binding site. Since the majority of the protections from chemical modification reside in proximity of H69, a model of *H. marismortui* 50S has been built with the implementation of H69. This model also shows the position of L14, one of the very few proteins present in this region of the 50S subunit (Figure 8a). The homology model of *S. solfataricus* aIF6 has been realized using the structure of the homologous *M. jannaschii* aIF6 (13), for which the high degree of sequence identity (44%) promises a good structure prediction. The docking of the aIF6 on the 50S subunit was realized using the constraints imposed by the RNA protection data and by the spatial relationship with L14.

aIF6 is a truncated cone with the two ring-shaped faces having different diameters and distinct properties. Groft and colleagues (13), analyzing the chemical properties of eIF6 and aIF6, proposed that the C-terminal side of this protein (smaller ring) was the ribosome
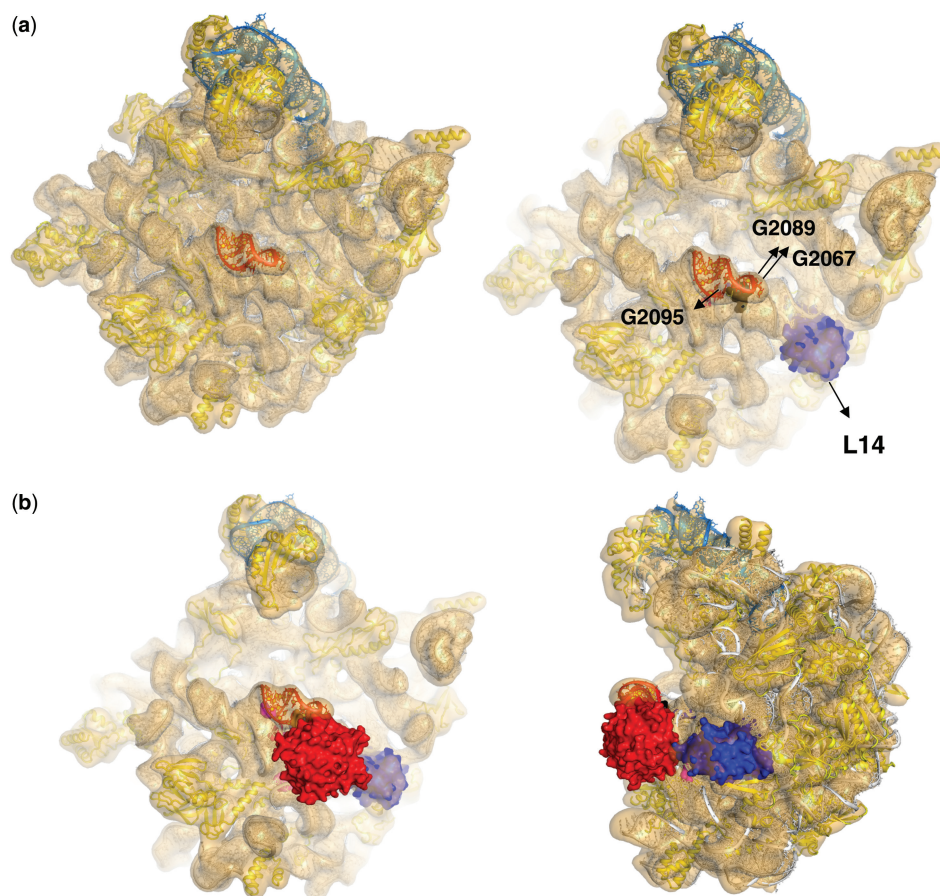
Figure 8. H69 modelling and docking of aIF6 on *H. marismortui* 50S. Cartoon and surface representations of *Haloarcula marismortui* 50S structure. (**a**, left) H69, in red, has been modeled using the structure of prokaryotic H69 (taken from the file 2I2V.pdb2) (19) using the programs Assemble and Pymol. (a, right) Nucleotides surrounding H69 protected by aIF6 are indicated by arrows; L14 is represented in dark blue solid surface. (**b**, left) H69, in red. aIF6 (solid red surface) has been docked using the constraints imposed by the protection of the 23S nucleotides and by the binding with L14 (blue solid surface). (b, right) Same, but rotated 80° around the Y axe.

interacting surface. Indeed, the high degree of sequence conservation and the charge distribution of this face of e/aIF6 may favor this hypothesis. In contrast with these observations, more recently, Menne and colleagues (9) using an automated yeast genetics platform, mapped on the opposite face of eIF6 (larger ring) all the residues that are important to stabilize the interaction of the protein with the 60S ribosome. Several of these residues are conserved between eukaryotes and archaea. On the strength of this factual information, in our model we therefore position the larger ring of aIF6 facing the 50S subunit. However, it should be kept in mind that the opposite orientation cannot be entirely ruled out at present.

The close vicinity of the 23S rRNA bases protected by bound aIF6 to the L14 binding pocket on the large ribosomal subunit (Figure 8a, right panel) strongly supports our docking model (Figure 8b). To orient the protein on the ribosome more precisely, we moved aIF6 closer to ribosomal protein L14. Furthermore, an analysis of the surface of the modelled aIF6 structure by meta-PPISP (30) revealed predicted patches for protein–protein interaction (data not shown). These regions are mainly located on a side of the putative ribosome binding surface and on the adjacent region of the lateral surface (residues 75–85).

In our docking model on the 50S subunit we tentatively position aIF6 so that the protection of the nucleotides around H69 can be obtained, conveniently orienting the ring so that the L14-aIF6 contacts would involve the patch of residues on the large ring and the lateral portion of aIF6 (Figure 8b). This fit also exposes the small ring face of aIF6 on the surface of the 50S, where it could be accessible to other possible interacting partners, as for instance the product of the archaeal homologue of the sdo1 gene that may modulate aIF6 function and its affinity for the 50S subunit (9).

DISCUSSION

The protein known as translation factor IF6 is shared specifically by the Archaea and the Eukarya, to the exclusion of Bacteria. Its function and properties have been studied to some extent in the eukaryotes, but remain somewhat elusive. Studies of eIF6-deficient yeast cells have suggested that the main role of the factor concerns the biogenesis of 60S ribosomes (3,4). In mammals, however, eIF6 seems to be important in translational regulation as its release from the 60S ribosomes is controlled by mitogen-activated kinases (10) and its depletion in

heterozygous knockout mice depresses translation initiation in certain organs (31). Other described functions of eIF6 regard its association with cytoskeletal proteins (32,33) an its involvement mi-RNA mediated post-transcriptional gene silencing (11). Thus, eIF6 seems to be a very important regulatory protein, possibly having multiple functions in eukaryotic cells.

In this work we show that the archaeal IF6 homologue (aIF6) is, at least *in vitro*, a potent inhibitor of translation that interacts strongly and specifically with the 50S ribosomal subunits hindering their association with the 30S particles and thereby the formation of 80S ribosomes. That aIF6 may function also *in vivo* as a translational repressor under unfavourable conditions is suggested by the fact that it is over-expressed upon both cold- and heat-shock (this work and ref. 26). Whether aIF6 also has a function in ribosome synthesis remains at present an open question; however, several lines of evidence indicate that this may not be the case. First, aIF6 is expressed at about the same level in different growth phases of *S. solfataricus* cells, while a ribosome synthesis factor is expected to be upregulated during exponential growth. Second, aIF6 is over-expressed upon thermal shock, a circumstance in which most ribosomal genes are downregulated. Third, aIF6 is present in sub-stoichiometric amounts with respect to the 50S subunits (about 1:10), but the aIF6 binding site remains available on the entire cellular pool of large ribosomal particles, which is not expected if aIF6 dissociation is a final step in large subunit maturation. Although many aspects of aIF6 function remain to be worked out, the present data suggest that the protein may have evolved in the archaeal/eukaryal lineage to fulfil a main role in translational regulation. Eukaryal IF6 may then have acquired additional functions during the evolution of the eukaryotic domain.

To get a deeper insight into the function of aIF6, we have mapped here for the first time its binding site on the large ribosomal subunits. According to our data, aIF6 lies in the centre of the 30S-interacting side of the 50S particle. The 23S rRNA bases protected by bound aIF6 are all located within the domain IV of 23S RNA, clustered in the vicinity of helix 69 and close to one another in the tertiary structure. Helix 69 in bacterial ribosomes is well known as a key region for subunit interaction. Notably, the 30S-interacting surface of the large subunits is very protein-poor and composed primarily of RNA. However, L14, shown here to contact aIF6, is one of the few proteins found in this ribosomal area (29) and is probably the main, if not the only, large subunit protein involved in subunit interaction (34). L14–aIF6 interaction appears to be quite strong: the two proteins form a complex even off the ribosome and upon immunoprecipitation aIF6 gets detached from the ribosome carrying along L14.

The experimental data obtained have been integrated in a model showing the docking of aIF6 in the 'palm' of the 50S subunit. This model provides a straightforward visual explanation of the aIF6 ability to inhibit subunits joining. In fact, of the 12 bridges stabilizing the interaction between 50S and 30S particles (35), seven form a triangular core acting as nucleation cluster for 70S formation (Figure 9a). The formation of these bridges is a
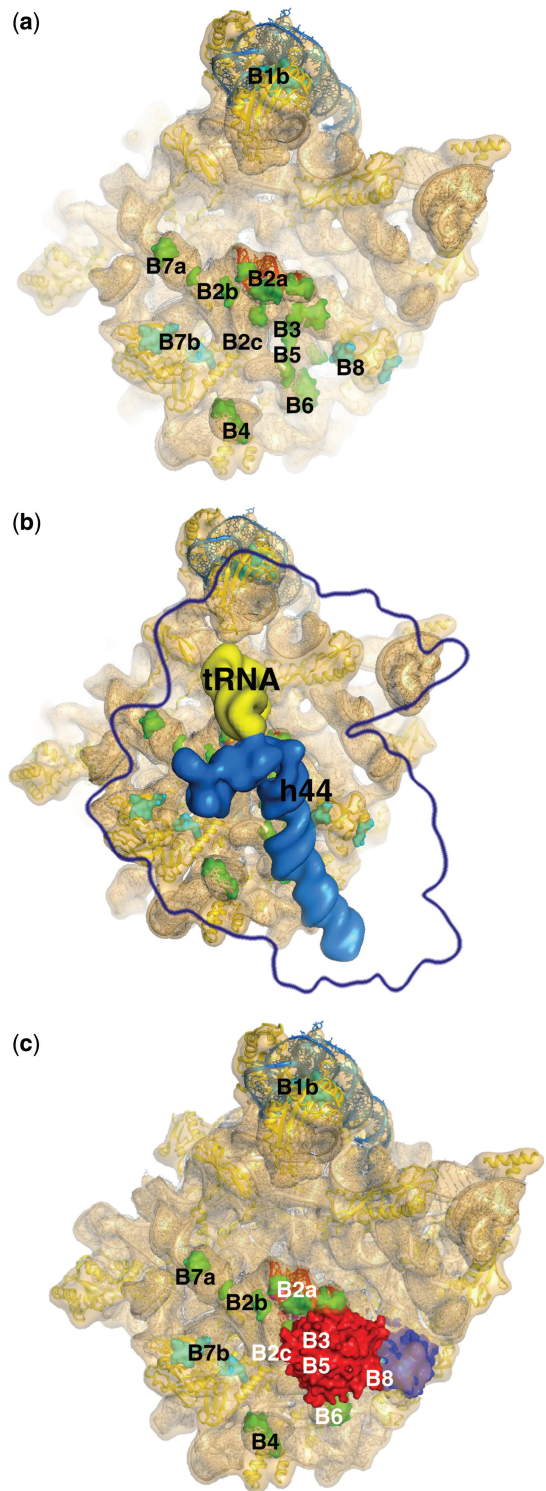

Figure 9. Structural details of aIF6 anti-association function. Cartoon and surface representations of *H. marismortui* 50S structure as in Figure 7. (**a**) Intersubunit bridges anchoring the 30S subunit to the 50S. H69, in red. Green and cyan surface representations are 50S nucleotides and amino acids, respectively, involved in bridging the 30S subunit. (**b**) Representation of docked 30S Initiation Complex. *Thermus thermophilus* 70S X-ray structure (35) has been used to position the silhouette of the 30S subunit (blue profile), h44 (blue solid surface) and the initiator tRNA (yellow solid surface). (**C**) aIF6 prevent 70S association. The docking of aIF6 on the *H. marismortui* 50S prevent the formation of the most important bridges between the two subunits.

prerequisite for the conformational changes of the 30S that are necessary to promote full association (Figure 9b; 36). aIF6 sits on the nucleation core, effectively preventing the formation of the most important contacts between the two subunits by steric hindrance (Figure 9c).

A very important question regards the mechanism controlling the binding/dissociation of aIF6 to the large ribosomal subunit, which in eukaryotes seems to vary depending on the organism. In yeast, eIF6 release requires the action of a GTPase (Efl1) aided by the docking protein Sdo1 (9). In mammals, eIF6 release is apparently triggered by site-specific phosphorylation of the factor (10). We show here that in *S. solfataricus* a fraction of 50S-bound aIF6 is released following translational activation. Interestingly, the dissociation of aIF6 from the ribosome is consistently accompanied by the appearance of a slower-migrating form of the protein, which cannot be accounted for by phosphorylation, as its mobility and appearance are unaffected by phosphatase treatment. We surmise that the slower-migrating form of aIF6 may result from an as yet unidentified chemical modification; this does not exclude, however, that aIF6 may also be phosphorylated as its eukaryal counterpart. The mechanism of aIF6 binding and release is currently being investigated in our laboratory.

SUPPLEMENTARY DATA

Supplementary Data are available at NAR Online.

ACKNOWLEDGEMENT

FUNDING

REFERENCES

1. Russell,D.W. and Spremulli,L.L. (1979) Purification and characterization of a ribosome dissociation factor (eukaryotic initiation factor 6) from wheat germ. *J. Biol. Chem.*, **254**, 8796–8800.
2. Valenzuela,D.M., Chaudhuri,A. and Maitra,U. (1982) Eukaryotic ribosomal subunit anti-association activity of calf liver is contained in a single polypeptide chain protein of Mr = 25,500 (eukaryotic initiation factor 6). *J. Biol. Chem.*, **257**, 7712–7719.
3. Basu,U., Si,K., Warner,J.R. and Maitra,U. (2001) The Saccharomyces cerevisiae TIF6 gene encoding translation initiation factor 6 is required for 60S ribosomal subunit biogenesis. *Mol. Cell Biol.*, **21**, 1453–1462.
4. Si,K. and Maitra,U. (1999) The Saccharomyces cerevisiae homologue of mammalian translation initiation factor 6 does not function as a translation initiation factor. *Mol. Cell Biol.*, **19**, 1416–1426.
5. Basu,U., Si,K., Deng,H. and Maitra,U. (2003) Phosphorylation of mammalian eukaryotic translation initiation factor 6 and its Saccharomyces cerevisiae homologue Tif6p: evidence that phosphorylation of Tif6p regulates its nucleocytoplasmic distribution and is required for yeast cell growth. *Mol. Cell Biol.*, **23**, 6187–6199.
6. Senger,B., Lafontaine,D.L., Graindorge,J.S., Gadal,O., Camasses,A., Sanni,A., Garnier,J.M., Breitenbach,M., Hurt,E. and Fasiolo,F. (2001) The nucle(ol)ar Tif6p and Efl1p are required for a late cytoplasmic step of ribosome synthesis. *Mol. Cell*, **8**, 1363–1373.
7. Fromont-Racine,M., Senger,B., Saveanu,C. and Fasiolo,F. (2003) Ribosome assembly in eukaryotes. *Gene*, **313**, 1–42.
8. Graindorge,J.S., Rousselle,J.C., Senger,B., Lenormand,P., Namane,A., Lacroute,F. and Fasiolo,F. (2005) Deletion of EFL1 results in heterogeneity of the 60 S GTPase-associated rRNA conformation. *J. Mol. Biol.*, **352**, 355–369.
9. Menne,T.F., Goyenechea,B., Sanchez-Puig,N., Wong,C.C., Tonkin,L.M., Ancliff,P.J., Brost,R.L., Costanzo,M., Boone,C. and Warren,A.J. (2007) The Shwachman-Bodian-Diamond syndrome protein mediates translational activation of ribosomes in yeast. *Nat. Genet.*, **39**, 486–495.
10. Ceci,M., Gaviraghi,C., Gorrini,C., Sala,L.A., Offenhauser,N., Marchisio,P.C. and Biffo,S. (2003) Release of eIF6 (p27BBP) from the 60S subunit allows 80S ribosome assembly. *Nature*, **426**, 579–584.
11. Chendrimada,T.P., Finn,K.J., Ji,X., Baillat,D., Gregory,R.I., Liebhaber,S.A., Pasquinelli,A.E. and Shiekhattar,R. (2007) MicroRNA silencing through RISC recruitment of eIF6. *Nature*, **447**, 823–828.
12. Gandin,V., Miluzio,A., Barbieri,A.M., Beugnet,A., Kiyokawa,H., Marchisio,P.C. and Biffo,S. (2008) Eukaryotic initiation factor 6 is rate-limiting in translation, growth and transformation. *Nature*, **455**, 684–688.
13. Groft,C.M., Beckmann,R., Sali,A. and Burley,S.K. (2000) Crystal structures of ribosome anti-association factor IF6. *Nat. Struct. Biol.*, **7**, 1156–1164.
14. Londei,P., Altamura,S., Cammarano,P. and Petrucci,L. (1986) Differential features of ribosomes and of poly(U)-programmed cell-free systems derived from sulphur-dependent archaebacterial species. *Eur. J. Biochem.*, **157**, 455–462.
15. Caserta,E., Tomsic,J., Spurio,R., La Teana,A., Pon,C.L. and Gualerzi,C.O. (2006) Translation initiation factor IF2 interacts with the 30 S ribosomal subunit via two separate binding sites. *J. Mol. Biol.*, **362**, 787–799.
16. Merryman,C. and Noller,H. F. (1998) *Footprinting and Modification-Interference Analysis of Binding Sites on RNA.*, Oxford University Press, Oxford, UK.
17. La Teana,A., Gualerzi,C.O. and Dahlberg,A.E. (2001) Initiation factor IF 2 binds to the alpha-sarcin loop and helix 89 of Escherichia coli 23S ribosomal RNA. *RNA*, **7**, 1173–1179.
18. Klein,D.J., Schmeing,T.M., Moore,P.B. and Steitz,T.A. (2001) The kink-turn: a new RNA secondary structure motif. *EMBO J.*, **20**, 4214–4221.
19. Berk,V., Zhang,W., Pai,R.D. and Cate,J.H. (2006) Structural basis for mRNA and tRNA positioning on the ribosome. *Proc. Natl Acad. Sci. USA*, **103**, 15830–15834.
20. Plewniak,F., Bianchetti,L., Brelivet,Y., Carles,A., Chalmel,F., Lecompte,O., Mochel,T., Moulinier,L., Muller,A., Muller,J. *et al.* (2003) PipeAlign: a new toolkit for protein family analysis. *Nucleic Acids Res.*, **31**, 3829–3832.
21. Guex,N., Diemand,A. and Peitsch,M.C. (1999) Protein modelling for all. *Trends Biochem. Sci.*, **24**, 364–367.
22. Marti-Renom,M.A., Stuart,A.C., Fiser,A., Sanchez,R., Melo,F. and Sali,A. (2000) Comparative protein structure modeling of genes and genomes. *Annu. Rev. Biophys. Biomol. Struct.*, **29**, 291–325.
23. Condo,I., Ciammaruconi,A., Benelli,D., Ruggero,D. and Londei,P. (1999) Cis-acting signals controlling translational initiation in the thermophilic archaeon Sulfolobus solfataricus. *Mol. Microbiol.*, **34**, 377–384.
24. Petrelli,D., LaTeana,A., Garofalo,C., Spurio,R., Pon,C.L. and Gualerzi,C.O. (2001) Translation initiation factor IF3: two domains, five functions, one mechanism? *EMBO J.*, **20**, 4560–4569.

25. Benelli,D., Maone,E. and Londei,P. (2003) Two different mechanisms for ribosome/mRNA interaction in archaeal translation initiation. *Mol. Microbiol.*, **50**, 635–643.

26. Tachdjian,S. and Kelly,R.M. (2006) Dynamic metabolic adjustments and genome plasticity are implicated in the heat shock response of the extremely thermoacidophilic archaeon Sulfolobus solfataricus. *J. Bacteriol.*, **188**, 4553–4559.

27. Merryman,C., Moazed,D., Daubresse,G. and Noller,H.F. (1999) Nucleotides in 23S rRNA protected by the association of 30S and 50S ribosomal subunits. *J. Mol. Biol.*, **285**, 107–113.

28. Martayan,A., Caprini,E. and Londei,P. (1993) The 23 S ribosomal RNA of Sulfolobus solfataricus strain MT4: sequence, structure and functional homology with other 23 S rRNAs of thermophilic, sulfur-dependent archaea. *Syst. Appl. Microbiol.*, **16**, 170–176.

29. Ban,N., Nissen,P., Hansen,J., Moore,P.B. and Steitz,T.A. (2000) The complete atomic structure of the large ribosomal subunit at 2.4 A resolution. *Science*, **289**, 905–920.

30. Qin,S. and Zhou,H.X. (2007) meta-PPISP: a meta web server for protein-protein interaction site prediction. *Bioinformatics*, **23**, 3386–3387.

31. Gandin,V., Miluzio,A., Barbieri,A.M., Beugnet,A., Kiyokawa,H., Marchisio,P.C. and Biffo,S. (2008) Eukaryotic initiation factor 6 is rate-limiting in translation, growth and transformation. *Nature*, **455**, 684–688.

32. Carotenuto,R., De Marco,N., Biffo,S., Wilding,M., Vaccaro,M.C., Marchisio,P.C., Capriglione,T., Russo,G.L. and Campanella,C. (2005) Phosphorylation of p27(BBP)/eIF6 and its association with the cytoskeleton are developmentally regulated in Xenopus oogenesis. *Cell Mol. Life Sci.*, **62**, 1641–1652.

33. Ceci,M., Offenhauser,N., Marchisio,P.C. and Biffo,S. (2002) Formation of nuclear matrix filaments by p27(BBP)/eIF6. *Biochem. Biophys. Res. Commun.*, **295**, 295–299.

34. Klein,D.J., Moore,P.B. and Steitz,T.A. (2004) The roles of ribosomal proteins in the structure assembly, and evolution of the large ribosomal subunit. *J. Mol. Biol.*, **340**, 141–177.

35. Yusupov,M.M., Yusupova,G.Z., Baucom,A., Lieberman,K., Earnest,T.N., Cate,J.H. and Noller,H.F. (2001) Crystal structure of the ribosome at 5.5 A resolution. *Science*, **292**, 883–896.

36. Hennelly,S.P., Antoun,A., Ehrenberg,M., Gualerzi,C.O., Knight,W., + Lodmell,J.S. and Hill,W.E. (2005) A time-resolved investigation of ribosomal subunit association. *J. Mol. Biol.*, **346**, 1243–1258.